SCIENTIA PLENA
www.scientiaplena.org.br
VOL. 22, NUM. 04 2026
doi: 10.14808/sci.plena.2026.044601

Effect of the ethanolic extract of *Anadenanthera colubrina* on the healing of excisional skin wounds

Efeito do extrato etanólico de *Anadenanthera colubrina* na cicatrização de feridas cutâneas excisionais

W. de S. Neres[1]; J. M. D. A. Aragão[1]; A. C. S. Nascimento[1]; J. F. Santos[2]; S. S. Matos[3]; D. A. de Souza[1]; J. M. F. Neto[2]; M. C. Duarte[3]; V. S. M. Junior[4]; C. B. Correa[2]; E. A. Camargo[1]; R. Grespan[1]*

[1]*Department of Physiology/Integrated Laboratory of Experimental Biology, Federal University of Sergipe, 49100-000, São Cristóvão - SE, Brazil*
[2]*Department of Morphology/Laboratory of Cancer and Leishmania Biology and Immunology, Federal University of Sergipe, 49100-000, São Cristóvão - SE, Brazil*
[3]*Department of Pharmacy, Federal University of Sergipe, 49100-000, São Cristóvão - SE, Brazil*
[4]*Gonçalo Moniz Institute – Fiocruz, Federal University of Bahia, 40296-710, Salvador - BA, Brazil*

**rgrespan@academico.ufs.br*
(Recebido em 10 de junho de 2025; aceito em 03 de março de 2026)

Anadenanthera colubrina has been widely used in traditional medicine as a healing agent. However, the current literature provides limited support for the use of this extract in wound healing. We investigated the effects of the ethanolic extract of *Anadenanthera colubrina* (EE*Ac*) on L929 fibroblasts, its antioxidant potential, and its wound healing properties using an excisional skin wound model in mice. Female Swiss mice were assigned to a control group (0.9% saline), a vehicle group (2% DMSO in propylene glycol), or an EE*Ac* group (5%). Treatments were applied topically once daily until the wounds were fully healed. EE*Ac* contains caffeic acid as its main compound, exhibits a high total phenolic content, and demonstrates strong antioxidant capacity against free radicals (ABTS, DPPH, and FRAP assays). Additionally, it was not cytotoxic to L929 fibroblasts. *In vivo*, the wound healing effect of EE*Ac* was demonstrated by a reduction in wound area and increased collagen deposition. These effects were accompanied by anti-inflammatory activity, evidenced by reduced myeloperoxidase levels during the inflammatory phase and decreased N-acetyl-*β*-D-glucosaminidase activity, in contrast with increased IL-10 levels during the proliferative phase. Taken together, our findings demonstrate that EE*Ac* enhances skin wound healing by modulating the inflammatory response and increasing collagen deposition without causing fibroblast toxicity.
Keywords: skin wound, inflammation, traditional medicine.

Anadenanthera colubrina tem sido amplamente usada na medicina tradicional como um agente de cura. No entanto, o corpo de evidências que apoiam o uso deste extrato para a cicatrização de feridas permanece limitado. Investigamos os efeitos do extrato etanólico de *Anadenanthera colubrina* (EE*Ac*) em fibroblastos L929, potencial antioxidante e suas propriedades de cicatrização de feridas usando um modelo de ferida cutânea excisional em camundongos. Camundongos Swiss fêmeas foram designados para um grupo controle (0,9% salina), veículo (2% DMSO em propilenoglicol) ou EEAc (5%). Os tratamentos foram aplicados topicamente uma vez ao dia até que as feridas estivessem completamente curadas. EE*Ac* contém ácido cafeico como seu principal composto, exibe um alto conteúdo fenólico total e demonstra forte capacidade antioxidante contra radicais livres (ensaios ABTS, DPPH e FRAP). Além disso, não foi citotóxico para fibroblastos L929. *In vivo*, o efeito de cicatrização de feridas do EE*Ac* foi demonstrado por uma redução na área da ferida e aumento da deposição de colágeno. Esses efeitos foram acompanhados por atividade anti-inflamatória, por níveis reduzidos de mieloperoxidase durante a fase inflamatória e atividade reduzida de N-acetil-*β*-D-glucosaminidase, em contraste com um aumento nos níveis de IL-10 durante a fase proliferativa. Tomados em conjunto, nossos achados demonstram que o EEAc melhora a cicatrização de feridas na pele modulando a resposta inflamatória e aumentando a deposição de colágeno sem causar toxicidade em fibroblastos.
Palavras-chave: pele, inflamação, medicina tradicional.

1. INTRODUCTION

Skin wounds are characterized by the disruption of skin integrity due to tissue damage [1], initiating a complex wound healing process. This process involves various cellular and molecular interactions to restore the skin and form a scar. The wound healing process typically consists of four overlapping phases: hemostasis, inflammation, proliferation, and remodeling [2]. The inflammatory phase, in particular, has been considered a key event in the repair of skin injuries. However, an exacerbated and persistent inflammatory response can impair healing, leading to complications such as chronic wounds [3, 4].

Wound treatment is commonly carried out due to the possibility of complications such as severe pain, hypertrophic scars, keloids, infections, amputations, sepsis, and death [5, 6]. Chronic wounds, in particular, represent significant economic burdens, with treatment in the United States alone costing approximately US$25 billion annually [7]. Although several conventional wound treatment methods are available, they often face limitations such as limited accessibility, high costs, and concerns regarding safety and effectiveness [8, 9]. As a result, the development of cost-effective alternative therapies has become increasingly important, particularly in relation to the use of herbal treatments [10].

Anadenanthera colubrina, commonly known as Angico, is a plant highly regarded for its medicinal properties in regions where it is native [11]. It has been widely used in traditional medicine, particularly for its supposed healing and anti-inflammatory effects [12]. Among its various parts, the bark is the most commonly used, known for its rich content of tannins and flavonoids [13, 14]. Studies conducted by Pessoa et al. (2012) [15] identified several bioactive compounds in the bark of *A. colubrina*, including condensed proanthocyanidins, leucoanthocyanidins, reducing sugars, flavonoids (such as quercetin glycosides), saponins, triterpenes, and steroids. These metabolites are associated with a range of beneficial properties, including anti-inflammatory activities [16], antioxidant [17] and antimicrobial [18]. According to Weber et al. (2011) [19] *A. colubrina* has considerable therapeutic potential. Although it is widely studied from ethnobotanical and economic perspectives, its pharmacological properties remain underexplored.

The healing effects of *A. colubrina* bark extract on excisional wounds in rats have been previously examined [15, 20]. However, evidence remains limited regarding its effects in murine skin wound models, and the mechanisms underlying its potential wound-healing activity are not fully understood. Therefore, further preclinical studies are warranted to assess its efficacy and to investigate inflammatory and remodeling-related pathways involved in skin repair [12,21]. Given these considerations, the investigation of the effects of the ethanolic extract of *A. colubrina* on the healing of excisional skin wounds induced in mice is justified.

Therefore, we evaluated the effects of EE*Ac* on fibroblasts *in vitro* and on excisional wound repair in mice. Overall, EE*Ac* showed antioxidant activity and did not reduce fibroblast viability under the conditions tested. *In vivo*, the findings suggest that EE*Ac* supports wound repair, with effects consistent with modulation of inflammatory responses and increased collagen deposition. Taken together, this study provides preclinical evidence supporting the wound-healing potential of EE*Ac* and may inform the development of alternative approaches for wound management.

2. MATERIALS AND METHODS

2.1 Plant Material

The bark of an adult tree of *Anadenanthera colubrina* (Vell.) Brenan var. *cebil* (Griseb.) Altschul (Fabaceae) was collected in November 2018, during the dry season, in the municipality of Monte Alegre de Sergipe, Sergipe, Brazil (10° 2' 44" S and 37° 35' 4" W). The species was authenticated by Dr. Marcus Vinicius Meiado and deposited in the Herbarium of the Federal University of Sergipe (ASE no. 42361).

2.1.1 Preparation of the Plant Extract

The bark was dried at 40°C (±2) for 72 hours, ground, and weighed, yielding 1.1 kg of powder. This material underwent exhaustive maceration in absolute ethanol for 72 hours, a process repeated three consecutive times. The resulting liquid was filtered and subjected to rotary evaporation at 45°C (Fisatom®, São Paulo/SP, Brazil). The resulting dry extract (338 g) was stored at 2–8°C. For formulation purposes, 5 g of the extract were diluted in 100 mL of a vehicle composed of 2% Dimethyl Sulfoxide (DMSO; Merck, Brazil) in Propylene Glycol (PG) [22] resulting in a 5% Ethanolic Extract of *Anadenanthera colubrina* (EE*Ac*) [15,20]. The powdered extract was stored at a temperature of 2–8 °C, protected from light. The formulation was prepared daily and kept under the same conditions until the time of treatment.

2.1.2 Characterization of EEAc by HPLC

The EE*Ac* was diluted with methanol to a concentration of 5 mg/mL, both extract solutions were sonicated for 30 minutes in an ultrasonic bath and filtered through membrane filters (PTFE – 0.45 µm) prior to injection into a High-Performance Liquid Chromatography system coupled with a Diode-Array Ultraviolet Detector (HPLC-DAD-UV).

HPLC-DAD-UV analyses were performed using a high-performance liquid chromatography system consisting of a DGU-20A3 degasser, two LC-20AD pumps, an SIL-20A HT autosampler, a CTO-20A column oven, an SPDM20Avp diode-array detector (DAD), and a CBM-20A system controller (Shimadzu Co., Kyoto, Japan). Chromatographic separation was carried out using a Shimadzu ODS analytical column (180 × 4.6 mm, particle size 5 µm), equipped with a Shimadzu ODS guard cartridge system (20 × 4 mm, particle size 5 µm). The mobile phase consisted of (A) ultrapure water with 1.0% acetic acid and (B) methanol. The flow rate was 0.8 mL/min and the sample injection volume was 20 µL.The elution gradient was as follows: 5% B (0.01–5 min); 5–15% B (5–12 min); 15–28% B (12–13 min); 28–28% B (12–13 min); 28–30% B (13–14 min); 30% B (14–22 min); 30–31% B (23–25 min); 31–32% B (25–35 min); 32% B (35–39 min); 33–34% B (40–45 min); 35–40% B (50–52 min), ending the analysis and returning to the initial conditions. The diode-array detector was set at 280 nm for chromatogram acquisition. Compound identification was based on comparison of absorption spectra and co-injection with standard substances (based on retention times). Standards of caffeic acid ($C_9H_8O_4$), chlorogenic acid ($C_{16}H_{18}O_9$), gallic acid ($C_7H_6O_5$), ferulic acid ($C_{10}H_{10}O_4$), myricetin ($C_{15}H_{10}O_8$), and quercetin ($C_{15}H_{10}O_7$) were obtained from Sigma-Aldrich® and prepared at a final concentration of 0.1 mg/mL in acetonitrile.

2.2 Total Phenolic Content Quantification

The methodology for determining the total phenolic content was based on the protocol proposed by Swain and Hillis (1959) [23], with modifications adapted for the microplate format. A 12 µL aliquot of the extract was pipetted in quadruplicate into a 96-well plate. Subsequently, 12 µL of Folin-Ciocalteu reagent and 200 µL of distilled water were added to each well. After a reaction time of 3 minutes, 25 µL of saturated sodium carbonate (Na_2CO_3) solution were introduced. The plate was then kept at room temperature and protected from light. After one hour, absorbance was measured using a spectrophotometer at 720 nm. The results were expressed as milligrams of gallic acid per gram of dry extract, determined using a standard curve with concentrations ranging from 25 to 200 µg/mL ($y = 0.0092x + 0.0385$; $R^2 = 0.9976$).

2.3 Experiments in vitro

2.3.1 Antioxidant Assays

In vitro tests were performed in triplicate to determine the antioxidant capacity of EE*Ac*. Extract concentrations used were 25, 50, 100, and 200 µg/mL, and the concentration required to inhibit half of the maximum evaluated parameter (IC50) was calculated. Trolox (Sigma Aldrich,

USA) was used as the antioxidant standard. The antioxidant capacity against the 2,2-diphenyl-1-picrylhydrazyl radical (DPPH; Sigma-Aldrich, USA) was measured by adding 50 µL of extract to 150 µL of DPPH at a concentration of 400 µM/L in a microplate. After 30 minutes of resting, protected from light, DPPH radical reduction was measured at 515 nm using a plate reader (Biotek, Synergy Mx).

The ABTS [2,2'-azino-bis(3-ethylbenzothiazoline-6-sulfonic acid)] radical assay was performed by adding 30 µL of the sample to a microplate, followed by the addition of 300 µL of the ABTS radical solution (1.25 mL of a 7 mM ABTS solution in 22 µL of a 140 mM potassium persulfate ($K_2S_2O_8$) solution). For these tests, the results were expressed as a percentage of inhibition [% inhibition = [(control − test)/control] × 100], based on absorbance values, from which the IC50 values were calculated.

The ferric reducing antioxidant power (FRAP) assay was conducted in a dark environment by adding 9 µL of each extract concentration in triplicate to a microplate, followed by 27 µL of distilled water and 270 µL of FRAP reagent, consisting of TPTZ, ferric chloride solution, and acetate buffer (0.3 M, pH 3.6) in a 1:1:10 ratio. The microplate was then incubated at 37 °C for 30 minutes. After incubation, absorbance was measured using a spectrophotometer at 595 nm. The results were expressed in µM Trolox equivalents, calculated using the equation $y = 0.0008x + 0.102$.

2.3.2 Cytotoxicity in Fibroblasts

The cell viability of the L929 fibroblast cell line was assessed using the colorimetric methylthiazolyl tetrazolium bromide (MTT) assay. The cell line was obtained from the Rio de Janeiro Cell Bank (BCRJ), Brazil. Cells were cultured in DMEM (Sigma Aldrich, USA) containing 10% fetal bovine serum (Life Technologies, India), 1% penicillin (Life Technologies, India)/streptomycin (Life Technologies, India), and maintained in a 5% CO_2 atmosphere at 37 °C. Fibroblasts were seeded in 96-well culture plates (2×10^4 cells/well) and treated with EE*Ac* at concentrations of 12.5, 25, 50, 100, and 200 µg/mL for 24 hours. MTT (0.5 mg/mL in phosphate-buffered saline (PBS)) was then added to the cells and incubated at 37 °C for 3 hours. After MTT removal, DMSO was added to solubilize the formazan crystals, and absorbance was measured at 570 nm. The assays were conducted in triplicate and normalized by considering the control absorbance as 100% cell viability.

2.4 Wound Healing model

Female Swiss albino mice (*Mus musculus*), nulliparous, healthy, weighing between 25–30 g, and aged between 8–12 weeks, were used. They were housed individually in polypropylene cages under controlled conditions: temperature of 21 ± 2 °C, humidity of 60 ± 5%, and a 12-hour light/dark cycle, with food and water provided *ad libitum*. All experimental procedures were conducted in accordance with the guidelines and standards established by the Animal Research Ethics Committee. The protocol was approved by the Animal Ethics Committee (CEPA) of the Federal University of Sergipe on March 25, 2019, under protocol number 07/2019.

Before wound induction, the animals underwent a seven-day acclimatization period. Ketamine (100 mg/kg, i.p.) and xylazine (10 mg/kg, i.p.) were used as anesthetic agents. After anesthesia, the dorsothoracic region was shaved, and antisepsis was performed with 0.5% chlorhexidine alcohol solution. Circular skin excision was performed using a 6 mm metal punch [24]. The animals were randomly assigned to three groups: control (treated with 0.9% sterile saline solution), vehicle (2% DMSO in PG), or EE*Ac*. Treatments were administered immediately after wound induction and repeated daily for 3, 7, or 14 days, depending on the experiment. Before administration, the treatments were homogenized to ensure standardization of the EEAc concentration applied to each animal. Each wound received 30 µL of the respective treatment (equivalent to 1.5 mg of EE*Ac* per wound/day). The 5% concentration was selected based on a previous study [15].

2.4.1 Wound Closure

Wounds were measured on days 0 (initial wound), 3, 7, and 14 using a digital caliper (n = 5–7/group). The wound area was calculated using the equation: Wound area (mm^2) = $\pi \times R \times r$, where $\pi = 3.1416$; R = the major radius and r = the minor radius. Wound closure was determined using the equation: Wound closure (%) = $(Wi - Wd) / Wi \times 100$, where Wi is the initial wound area and Wd is the wound area on the measured days [25]. After obtaining this parameter, the percentage of the wound area that remained open was calculated by subtracting the wound closure percentage from 100%.

2.4.2 Tissue Collection

The animals were euthanized using an overdose of ketamine (300 mg/kg, i.p.) and xylazine (30 mg/kg, i.p.). Animals were randomly allocated to treatment groups. Wound area was assessed longitudinally in the same animals on days 0, 3, 7, and 14. For tissue-based analyses, independent subsets of animals from each group were euthanized at predetermined time points (days 1, 3, 7, and 14). Full-thickness skin samples were collected using an 8-mm biopsy punch centered on the wound, including the wound bed and a margin of perilesional intact skin. A total of 103 mice were used for all analyses in this study.

2.5 Histopathological Analysis

Animals assigned to wound closure analysis (n = 5/group) were subjected to histological evaluation on the 14th day after injury. The tissues were bisected into two fragments, sectioned using a microtome (5 μm), and stained with Hematoxylin and Eosin (H&E) or Masson's Trichrome. Subsequently, tissue sections were examined (10 different areas) under an optical microscope (Nikon, Japan), and images were captured using a digital camera (Coolpix 4500, Roper Scientific, Japan). The researchers were kept blinded during wound collection, and the histological analysis was conducted blindly and independently by two researchers. A scoring scale ranging from 0 to 3 was used to evaluate several parameters, including leukocyte infiltration, vascularization, re-epithelialization, and collagen deposition. The scoring system was as follows: 0 for absent, 1 for mild, 2 for moderate, and 3 for marked [13].

2.6 Inflammatory Assays

2.6.1 Myeloperoxidase and N-acetyl-β-D-glucosaminidase Activity

Myeloperoxidase (MPO) activity was quantified to indirectly assess neutrophil infiltration on days 1, 3, and 7 of healing (n = 5–7/group/time point). Tissues were homogenized in PBS and 0.5% Hexadecyltrimethylammonium Bromide (HTAB 0.5%) at a ratio of 1 mL/100 mg of tissue. After homogenization, samples were centrifuged for 2 minutes at 14,000 rpm. A volume of 20 μL of the supernatant was used for reaction with 200 μL of O-dianisidine solution, and finally, sample absorbance was measured at 460 nm [26].

To indirectly determine macrophage infiltration in the lesions, N-acetyl-β-D-glucosaminidase (NAG) activity was quantified on days 1, 3, and 7 of the repair process (n = 5–7/group/time point). Tissue samples were homogenized in cytokine extraction buffer (PBS containing a protease inhibitor cocktail, phenylmethylsulfonyl fluoride (PMSF), sodium chloride (NaCl), ethylenediaminetetraacetic acid (EDTA), and Tween 20) and then centrifuged. The pellet was resuspended in a buffer containing 0.2% NaCl and 1.6% NaCl with 5% glucose. Subsequent steps involved homogenization, centrifugation, and resuspension of the pellet in 0.9% NaCl and 0.1% Triton X-100 (1:1). The supernatant was mixed with 0.767 mg/mL of p-nitrophenyl-N-acetyl-β-D-glucosaminide for the NAG assay. The plate was incubated at 37 °C for 30 minutes, and the reaction was stopped with a buffer containing 0.2 M glycine. Samples were analyzed at 405 nm. Finally, the result was normalized by tissue weight and expressed as Optical Density (OD)/100 mg of tissue [27]. All analyses were conducted in a blinded manner.

2.6.2 Cytokine Quantification

Tissue samples from days 1 and 3 of repair (n = 5–7/group/time point) were subjected to quantification of the cytokines TNF-α (Tumor Necrosis Factor–α) and IL-10 (Interleukin-10) using ELISA kits, following the manufacturer's protocol (Peprotech®, USA). All analyses were conducted in a blinded manner.

2.7 Statistical Analysis

Data were subjected to the Shapiro-Wilk normality test. Depending on the data distribution, one-way or two-way ANOVA with Bonferroni post hoc test was performed. When appropriate, the Kruskal-Wallis test was used with Dunn's post hoc test. Data were expressed as mean ± SEM or as median and interquartile range for histological parameter scores. Statistical analysis was performed using GraphPad Prism® 8.0 software, with $p < 0.05$ considered statistically significant.

3. RESULTS

3.1 Phytochemical Analysis

The chromatographic profile of EE*Ac* revealed the presence of several compounds in the extract, with caffeic acid specifically identified (Figure 1).

The total phenolic content of EE*Ac* was estimated using gallic acid as the standard. At a concentration of 500 µg/mL, the total phenolic content was found to be 168.02 ± 3.2 µg of gallic acid equivalent per mg of dry extract, calculated according to the standard curve described in the methodology.

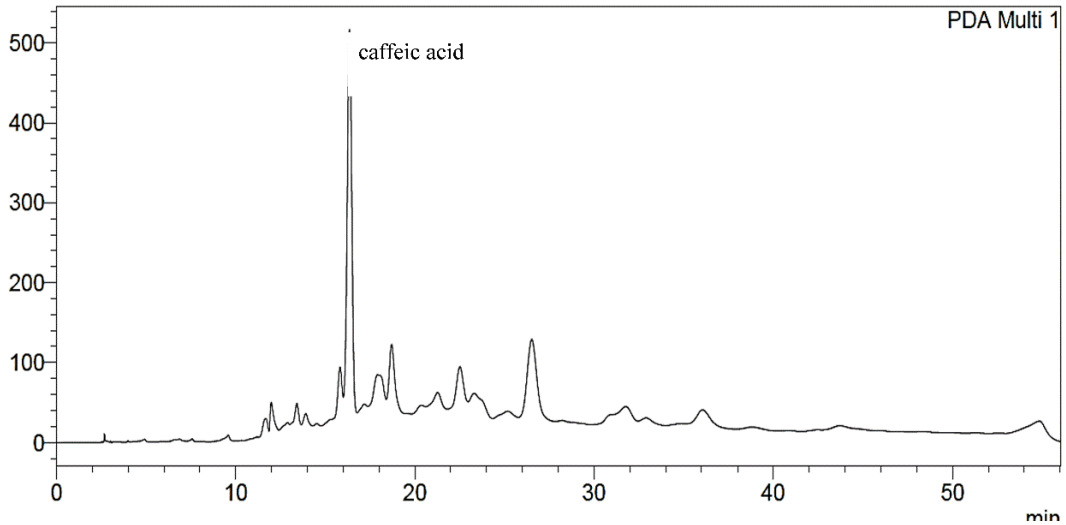

Figure 1. Extract Characterization by HPLC. Chromatograms were obtained by co-elution of EEAc with the standard using HPLC-DAD-UV (280 nm). Caffeic acid showed a retention time (Rt) of 16.8 min. In all chromatograms, the peak with Rt = 5.65 min showed a Peak Purity Index > 0.9999 (Laboratory Solution, Shimadzu).

3.2 Antioxidant Potential of EE*Ac*

To evaluate the antioxidant capacity of EE*Ac*, we conducted the DPPH, ABTS, and FRAP tests (Figure 2). In the DPPH radical scavenging assay, which is based on the hydrogen donor ac-ceptance by the DPPH compound from the antioxidant molecule, EE*Ac* showed an in-crease in the percentage of radical scavenging proportional to the concentration increase. At a concentration of 100 µg/mL, EE*Ac* presented a scavenging percentage similar to the standard,

and at the highest concentration, it showed a higher scavenging percentage than the standard ($p = 0.0007$). However, all concentrations of EE*Ac* and the standard (Trolox) had a greater antioxidant capacity than the system ($p < 0.0001$) (Figure 2a).

In the ABTS radical scavenging assay, EE*Ac* showed greater antioxidant activity starting from the concentration of 100 µg/mL of the extract, when compared to the standard (Trolox) ($p = 0.0002$). Similarly to the DPPH assay, all concentrations and the standard had higher antioxidant activity than the system ($p < 0.0001$) (Figure 2b).

Regarding FRAP, it was observed that the extract presented iron reduction activity in a concentration-response manner, reducing iron from its ferric form to the ferrous form (Figure 2c).

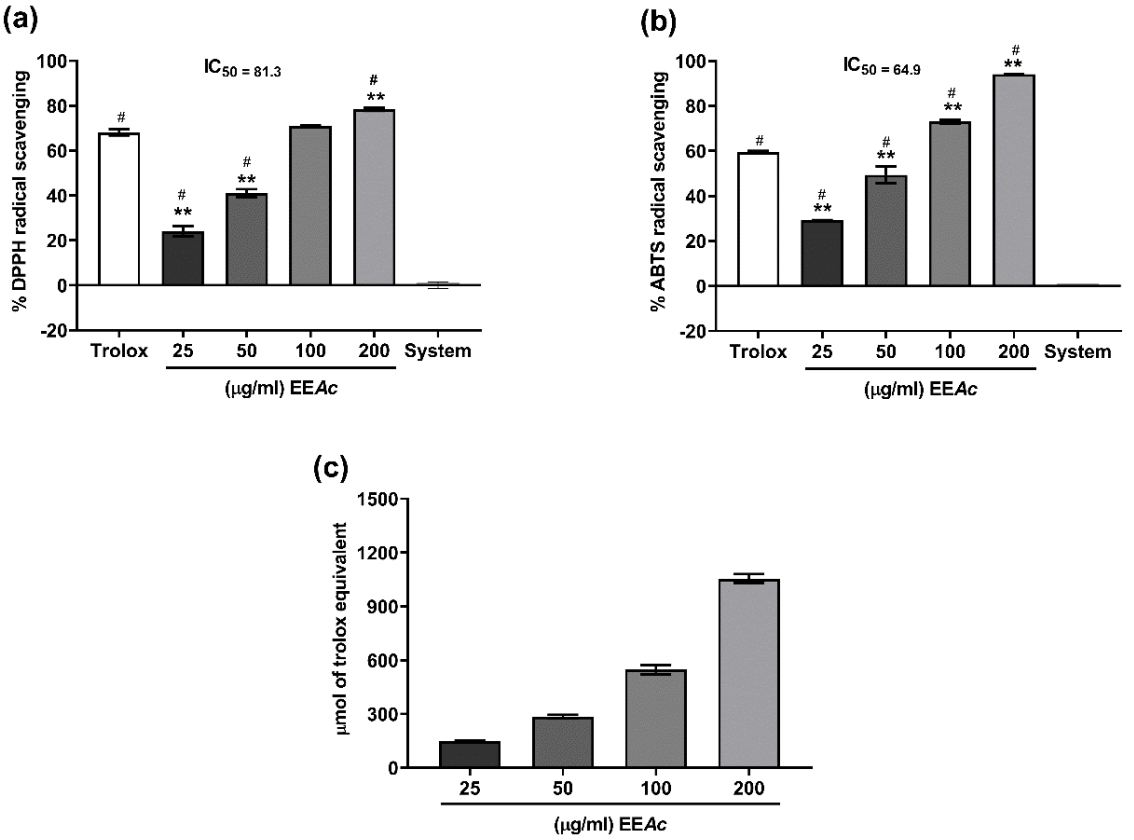

*Figure 2. Antioxidant Activity of EEAc. The assays for ABTS (a) and DPPH (b) radical scavenging capacity, as well as the FRAP assay (c), were conducted in triplicate. Results were expressed as mean ± SEM and analyzed by two-way ANOVA with Bonferroni post-test. Data with **$p < 0.001$ or #$p < 0.0001$ were considered significant compared to Trolox or the System, respectively.*

3.3 EEAc Does Not Exhibit Cytotoxicity in L929 Cells

The MTT assay was performed to evaluate the potential of EE*Ac* to support cell proliferation. In this assay, a decrease in metabolic activity eventually leads to apoptosis or necrosis, representing a reduction in cell viability. At all tested concentrations, fibroblast viability remained above 72% for L929 cells (Figure 3).

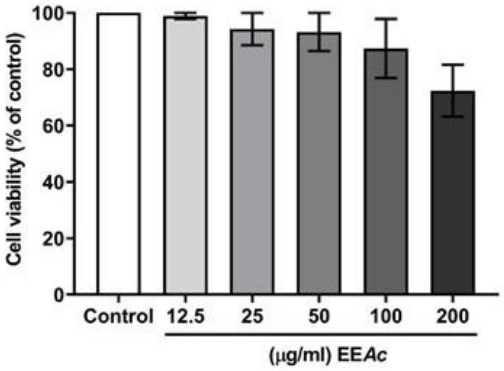

Figure 3. Cytotoxicity of EEAc on L929 Cell Lines. The assay was performed using MTT to evaluate the viability of L929 cells after treatment with the extract. Experiments were conducted in triplicate. Results were expressed as mean ± SEM, and analyzed using the Kruskal-Wallis test followed by Dunn's post-test.

3.4 EEAc Reduces the Area of Excisional Skin Wounds

The impact of EE*Ac* on wound healing progression was initially assessed by monitoring the percentage of open wound areas. On days 3 and 7, a significant reduction in the percentage of the wound area that remained open was observed in animals treated with EE*Ac*, in contrast to the control or vehicle groups ($p < 0.01$ on day 3 and $p < 0.001$ on day 7) (Figures 4a, b).

To further clarify these differences between groups, the results were also expressed as area under the curve (AUC). Notably, treatment with EE*Ac* led to a reduction in the open wound area, promoting closure. This was evidenced by the lower AUC observed exclusively in the treated group compared to the control ($p = 0.0132$) or vehicle ($p = 0.0068$) groups (Figure 4c).

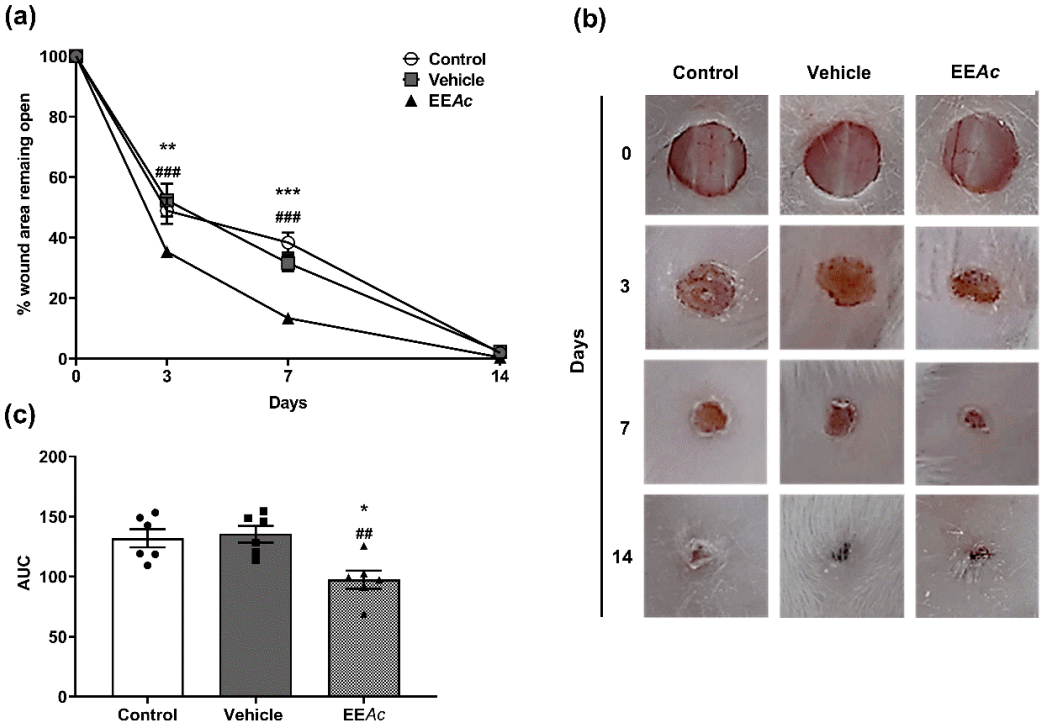

*Figure 4. Effect of EEAc on the Area of Excisional Skin Wounds Induced in Mice. Animals were topically treated and divided into three groups: control, vehicle, or EEAc (n = 5–7/group). The percentage of the wound area that remained open was calculated as 100% minus the wound closure percentage (a). The area under the curve (AUC) of the percentage of the open wound area is illustrated in photographs taken on days 0, 3, 7, and 14 (b) and presented quantitatively in (c).Results were expressed as mean ± SEM, and analyzed using two-way ANOVA with Bonferroni post-test. Data with *p < 0.05 or ##p < 0.01 vs. control or vehicle, respectively, were considered significant.*

3.5 EEAc Reduced MPO and Increased NAG in Healing Wounds

MPO is an enzyme released by neutrophils, which can serve as a marker of the presence of these cells in skin tissue [13]. Our study revealed that animals treated with EE*Ac* showed reduced MPO activity on day 3 compared to the control and vehicle groups ($p < 0.01$ and $p < 0.001$, respectively) (Figure 5a).

Indirect measure of macrophage infiltration was quantified by measuring the lysosomal enzyme NAG, which is highly expressed in activated macrophages [28]. An increase in NAG was observed on day 7 in the EEAc group compared to the control ($p = 0.0001$) and vehicle ($p = 0.0009$) groups (Figure 5b). In both analyses performed, no difference was observed between the control and vehicle groups.

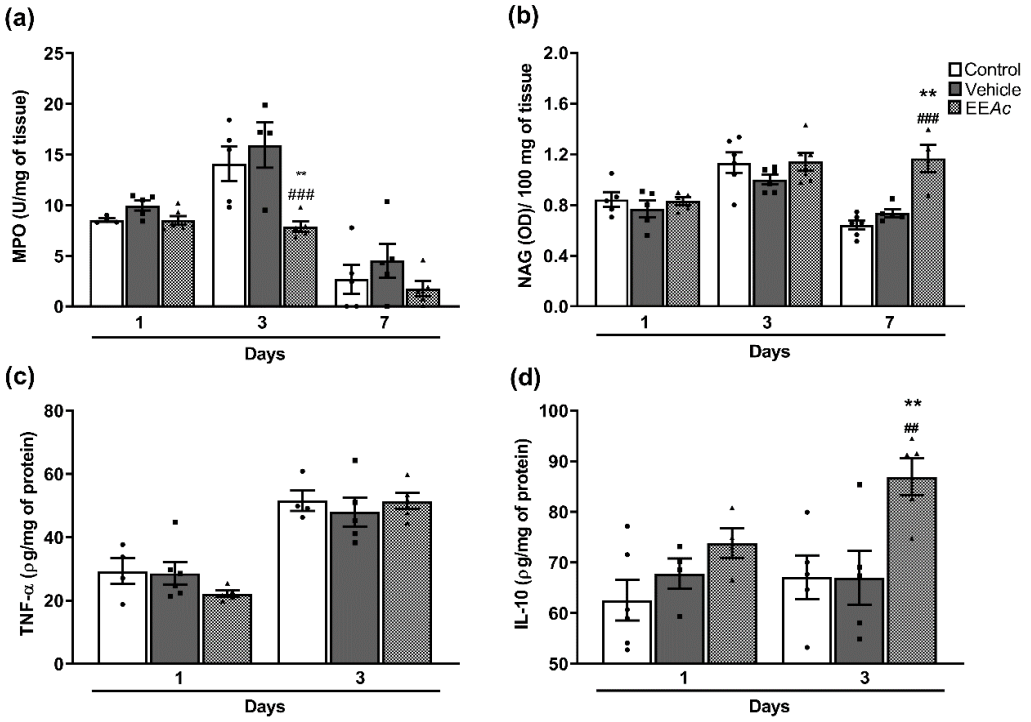

Figure 5. Anti-inflammatory effect of EEAc on excision-induced skin wounds in mice. The animals were topically treated and divided into three groups: control, vehicle, or EEAc (n = 5–7/group/time point). Lesions were collected on days 1, 3, and 7 to assess the activity of the MPO enzyme, represented as uMPO/mg of tissue (a), or the NAG enzyme, represented as OD/100 mg of tissue (Optical Density) (b). For cytokine quantification, lesions were collected on days 1 and 3 to measure TNF-α (c) and IL-10 (d), represented as pg/mg of protein. Results were expressed as mean ± SEM, analyzed by two-way ANOVA and Bonferroni post-test. Data with p<0.01 () and p<0.001 (*) or ###p<0.001 vs control or vehicle, respectively.

3.6 EEAc Has Anti-Inflammatory Potential

No significant difference was found in TNF concentration among the groups (Figure 5c). Nevertheless, IL-10 concentration increased in the group treated with EE*Ac*, observed on day 3, compared to the control and vehicle groups ($p < 0.01$) (Figure 5d).

3.7 EEAc Improves Collagen Deposition in Skin Lesions

Figure 6a shows histological images of the wound stained with H&E and Masson's Trichrome. The parameters of re-epithelialization, collagen deposition, leukocyte infiltration, and vascularization (Figures 6 b–e) were evaluated using a scoring system ranging from 0 to 3 to assess wound quality. We found an increase in the score only for collagen deposition in the EE*Ac* group compared to the control ($p = 0.0039$) and vehicle ($p = 0.0039$) groups.

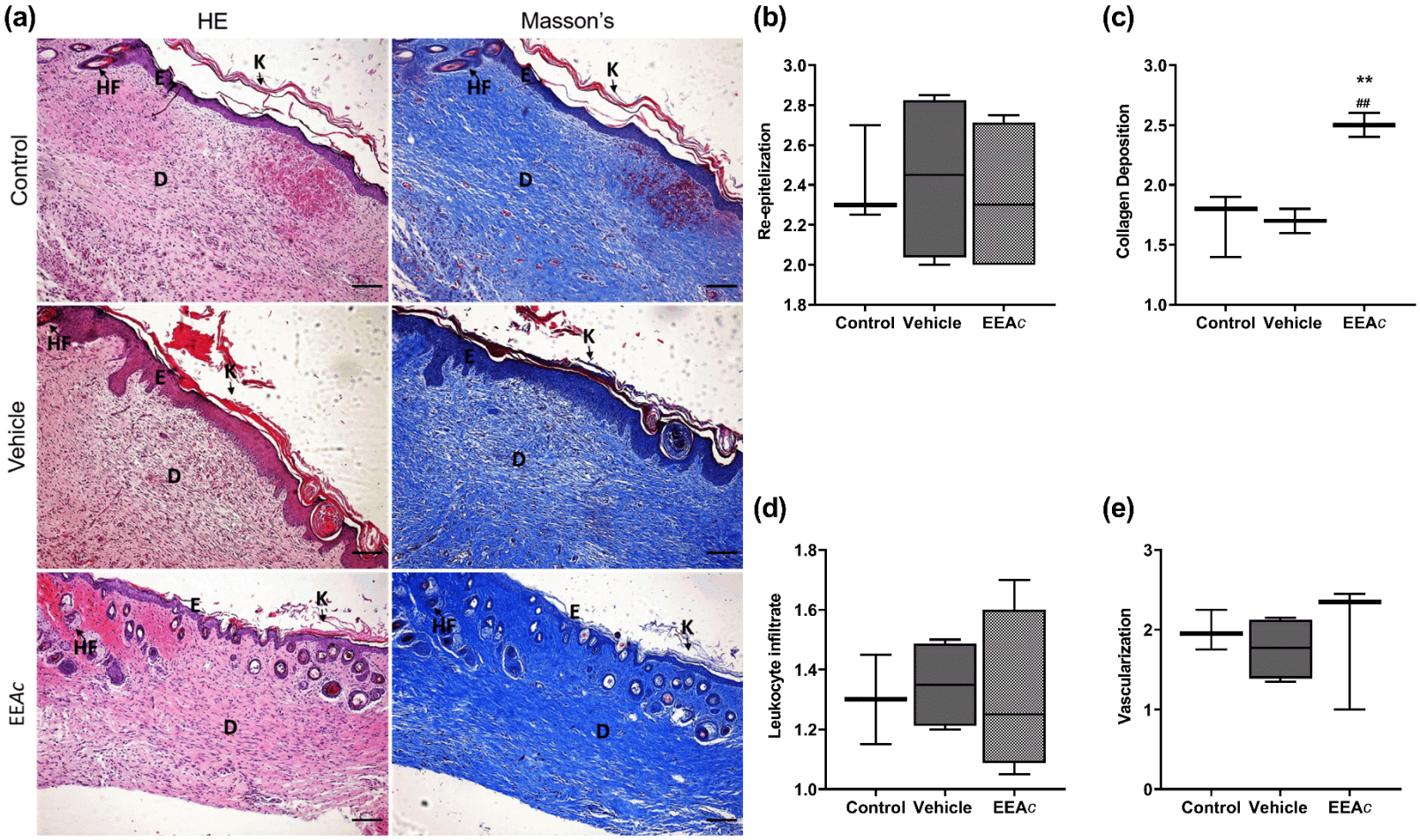

*Figure 6. Effect of EEAc on Histological Parameters of Excisional Skin Wounds Induced in Mice. Animals were topically treated and divided into three groups: control, vehicle, or EEAc (n = 5/group). Tissues were collected on day 14 of healing for histological analysis, and photomicrographs stained with (a) H&E and Masson's Trichrome, at 100x magnification (100 µm), show the control, vehicle, and EEAc groups, respectively. Histological specimens were analyzed for healing parameters: (b) re-epithelialization, (c) collagen deposition, (d) leukocyte infiltration, and (e) vascularization (n = 5/group). Results were expressed as median and interquartile range and analyzed by one-way ANOVA with Bonferroni post-test. Data with **p < 0.01 and ##p < 0.01 vs. control or vehicle, respectively, were considered significant. D – Dermis; E – Epidermis; HF – Hair follicle; K – Keratin.*

4. DISCUSSION

The healing effects of medicinal plants are closely associated with the presence of secondary compounds produced by the plant's metabolism, which typically induce an anti-inflammatory response [29,30]. For *A. colubrina*, its healing effect can be mainly attributed to the abundant presence of flavonoids and tannins in the bark [12, 14, 31]. In this study, the high total phenolic content and the presence of caffeic acid as an identified constituent are consistent with the observed biological effects and may contribute to the wound-healing profile of EE*Ac*. However, further studies using fractionation/standardization would be required to establish a direct causal relationship. Polyphenol-rich plants are closely linked to the inhibition of ROS (Reactive Oxygen Species) generation, serving as important antioxidants and modulating the release of pro-inflammatory cytokines and interleukins during the tissue repair process [32].

The *in vitro* antioxidant activity (DPPH/ABTS) suggests that EE*Ac* has redox-active constituents, which could plausibly support anti-inflammatory effects in vivo. However, antioxidant capacity in chemical assays does not directly demonstrate in vivo ROS modulation. Furthermore, its iron-reducing capacity could enhance antioxidant effects an activity linked to its flavonoid content [33]. Indeed, phenolic compounds present in plants, such as caffeic acid and the phenethyl ester derivative of caffeic acid, have been associated with various biological properties, including antibacterial and anti-inflammatory effects [34–36]. Moreover, the extract also demonstrated good viability in L929 fibroblasts. Collectively, these results indicate EE*Ac*'s potential as a treatment for skin wounds

The excisional wound model used in this study assessed the impact of EE*Ac* on acute lesions, enabling the determination of the degree of wound closure through secondary intention healing [37,38]. Our investigation demonstrated that EE*Ac* effectively reduced the area of excisional wounds during the 3- and 7-day healing periods. However, it did not accelerate the repair process by the end of the experimental period. This suggests that EE*Ac* predominantly exerted its activity during the inflammatory phase, likely due to the antioxidant and anti-inflammatory properties of *A. colubrina* [16].

It is important to note that while wound area measurement is a common practice, this parameter alone does not fully determine the efficacy of wound healing agents. As previously mentioned, phenolic compounds and flavonoids exhibit high antioxidant capacity due to their redox properties, which may play a key role in scavenging and neutralizing free radicals, ultimately contributing to their antiproliferative and anti-inflammatory effects [39].

Therefore, the quality of wound repair at the end of the experiment (day 14) was evaluated through histological analysis, revealing increased collagen deposition. However, no differences were observed in the parameters of leukocyte infiltration, vascularization, and re-epithelialization. Previous research by Pessoa et al. (2015) [20], evaluated the effect of *A. colubrina* bark extract on the healing of excisional skin wounds in rats. While no differences in wound area were observed, increased collagen deposition was also reported, which is consistent with the findings of the present study. These results suggest that *A. colubrina* may contribute to aspects of the tissue repair process, particularly those related to collagen deposition during healing.

Given the macroscopic and microscopic effects observed for EE*Ac*, we measured the cellular biomarkers MPO and NAG to evaluate neutrophil and macrophage accumulation, respectively. Neutrophils are associated with uncontrolled inflammation and impaired tissue repair [40], making them dispensable and detrimental to the healing process In contrast, macrophages play an indispensable role in wound healing. Studies have shown that macrophage depletion in mice is associated with reduced wound contraction, impaired re-epithelialization, diminished collagen deposition, and angiogenesis, as well as increased neutrophil presence [41, 42]. Maintaining an M2 macrophage profile is crucial for proper tissue resolution [43].

In their study on the wound healing activity of the hydroethanolic extract from *Maytenus ilicifolia* leaves, de Moura et al. (2021) [45] reported similar findings: a reduction in MPO activity by day 3, followed by increased NAG activity by day 7. The authors proposed that this pattern reflects decreased neutrophil infiltration coupled with progressive macrophage recruitment over time, thereby promoting tissue repair progression.

Numerous natural products exhibit anti-inflammatory activity that supports wound healing, including TNF-α inhibition and/or IL-10 stimulation [30]. TNF-α amplifies inflammation by activating Nuclear Factor-κB (NF-κB) and inducing pro-inflammatory mediators such as IL-1β, IL-6, and TNF-α itself [44]. Consequently, TNF-α inhibition promotes wound closure, while its elevated levels impair healing [45, 46].

Alternatively, IL-10 has been linked to skin regeneration by reducing inflammation and promoting robust M2 polarization [47, 48]. Consistent with our findings, Amorim et al. (2017) [13] demonstrated that *Copaifera paupera* oleoresin enhances wound closure, increases collagen deposition, and elevates IL-10 levels in diabetic excisional wounds in mice. Although our study did not explore the correlation between IL-10 release and wound quality, emerging research highlights IL-10's "non-classical" role in wound repair Through its antifibrotic properties, IL-10 activates STAT3 (Signal Transducer and Activator of Transcription 3) signaling, thereby increasing hyaluronan (HA) content. This stimulates fibroblasts to synthesize an HA-rich pericellular matrix, ultimately promoting regenerative epithelial wound healing [49].

5. CONCLUSION

In conclusion, EE*Ac* showed antioxidant activity and did not reduce fibroblast viability under the conditions tested. In a murine excisional wound model, topical EEAc was associated with reduced open wound area at early time points and with an anti-inflammatory profile (reduced MPO activity and increased IL-10), alongside increased NAG activity (a macrophage-associated marker) and higher collagen deposition at day 14. Collectively, these findings support the wound-healing potential of *A. colubrina* bark extract and warrant further studies to confirm mechanisms and evaluate additional endpoints related to scar quality and treatment response.

6. ACKNOWLEDGMENTS

The authors gratefully acknowledge the financial support provided by the Brazilian Federal Agency for Support and Evaluation of Graduate Education (CAPES), the National Council for Scientific and Technological Development (CNPq), and the Federal University of Sergipe (UFS) for providing the infrastructure and funding necessary to conduct this research.

7. REFERENCES

1. Mahdavian Delavary B, van der Veer WM, van Egmond M, et al. Macrophages in skin injury and repair. Immunobiology. 2011;216:753-62. doi: 10.1016/j.imbio.2011.01.001
2. Mirza RE, Koh TJ. Contributions of cell subsets to cytokine production during normal and impaired wound healing. Cytokine. 2015;71:409-12. doi: 10.1016/j.cyto.2014.09.005
3. Gurtner GC, Werner S, Barrandon Y, et al. Wound repair and regeneration. Nature. 2008;453:314-21. doi: 10.1038/nature07039
4. Landén NX, Li D, Ståhle M. Transition from inflammation to proliferation: a critical step during wound healing. Cell Mol Life Sci. 2016;73:3861-85. doi: 10.1007/s00018-016-2268-0
5. Larouche J, Sheoran S, Maruyama K, et al. Immune regulation of skin wound healing: Mechanisms and novel therapeutic targets. Adv Wound Care (New Rochelle). 2018;7:209-31. doi: 10.1089/wound.2017.0761
6. Dwivedi D, Dwivedi M, Malviya S, et al. Evaluation of wound healing, anti-microbial and antioxidant potential of *Pongamia pinnata* in wistar rats. J Tradit Complement Med. 2017;7:79-85. doi: 10.1016/j.jtcme.2015.12.002
7. Sen CK, Gordillo GM, Roy S, et al. Human skin wounds: a major and snowballing threat to public health and the economy. Wound Repair Regen. 2009;17:763-71. doi: 10.1111/j.1524-475X.2009.00543.x
8. Duque APN, Pinto NCC, Mendes RF, et al. In vivo wound healing activity of gels containing *Cecropia pachystachya* leaves. J Pharm Pharmacol. 2016;68:128-38. doi: 10.1111/jphp.12496
9. Okonkwo UA, DiPietro LA. Diabetes and wound angiogenesis. Int J Mol Sci. 2017;18:1419. doi: 10.3390/ijms18071419

10. Pereira RF, Bártolo PJ. Traditional therapies for skin wound healing. Adv Wound Care (New Rochelle). 2016;5:208-29. doi: 10.1089/wound.2013.0506
11. Agra MF, Baracho GS, Nurit K, et al. Medicinal and poisonous diversity of the flora of "Cariri Paraibano", Brazil. J Ethnopharmacol. 2007;111:383-95. doi: 10.1016/j.jep.2006.12.007
12. Delices M, Muller JAI, Arunachalam K, et al. *Anadenanthera colubrina* (Vell) Brenan: Ethnobotanical, phytochemical, pharmacological and toxicological aspects. J Ethnopharmacol. 2023;300:115745. doi: 10.1016/j.jep.2022.115745
13. Amorim JL, Figueiredo JB, Amaral ACF, et al. Wound healing properties of *Copaifera paupera* in diabetic mice. PLoS One. 2017;12:e0187380. doi: 10.1371/journal.pone.0187380
14. Cartaxo SL, Souza MMA, de Albuquerque UP. Medicinal plants with bioprospecting potential used in semi-arid northeastern Brazil. J Ethnopharmacol. 2010;131:326-42. doi: 10.1016/j.jep.2010.07.003
15. Pessoa WS, Estevão LRM, Simões RS, et al. Effects of angico extract (*Anadenanthera colubrina* var. cebil) in cutaneous wound healing in rats. Acta Cir Bras. 2012;27:655-70. doi: 10.1590/s0102-86502012001000001
16. Santos JS, Marinho RR, Ekundi-Valentim E, et al. Beneficial effects of *Anadenanthera colubrina* (Vell.) Brenan extract on the inflammatory and nociceptive responses in rodent models. J Ethnopharmacol. 2013;148:218-22. doi: 10.1016/j.jep.2013.04.012
17. Gomes de Melo J, de Sousa Araújo TA, Thijan Nobre de Almeida e Castro V, et al. Antiproliferative activity, antioxidant capacity and tannin content in plants of semi-arid northeastern Brazil. Molecules. 2010;15:8534-42. doi: 10.3390/molecules15128534
18. De Araújo DRC, da Silva LCN, da Silva AG, et al. Comparative analysis of anti-*Staphylococcus aureus* action of leaves and fruits of *Anadenanthera colubrina* var. cebil (Griseb.) Altschul. Afr J Microbiol Res. 2014;8:2690-6. doi: 10.5897/AJMR2014.6901
19. Weber CR, Soares CML, Lopes ABD, et al. *Anadenanthera colubrina*: a therapeutic potential study Rev Bras Farm.2011;92:235-44.
20. Pessoa WS, Estevão LRM, Simões RS, et al. Fibrogenesis and epithelial coating of skin wounds in rats treated with angico extract (*Anadenanthera colubrina* var. *cebil*). Acta Cir Bras. 2015;30:353-8. doi: 10.1590/S0102-865020150050000007
21. Duraz AY, Khan SA. Knowledge, attitudes and awareness of community pharmacists towards the use of herbal medicines in muscat region. Oman Med J. 2011;26:451-3. doi: 10.5001/omj.2011.115
22. Gao M, Nguyen TT, Suckow MA, et al. Acceleration of diabetic wound healing using a novel protease-anti-protease combination therapy. Proc Natl Acad Sci USA. 2015;112:15226-31. doi: 10.1073/pnas.1517847112
23. Swain T, Hillis WE. The phenolic constituents of *Prunus domestica* . I.—The quantitative analysis of phenolic constituents. J Sci Food Agric 1959;10:63-8. doi: 10.1002/jsfa.2740100110
24. Canesso MCC, Vieira AT, Castro TBR, et al. Skin wound healing is accelerated and scarless in the absence of commensal microbiota. J Immunol. 2014;193:5171-80. doi: 10.4049/jimmunol.1400625
25. Pinto NCC, Cassini-Vieira P, de Souza-Fagundes EM, et al. *Pereskia aculeata* Miller leaves accelerate excisional wound healing in mice. J Ethnopharmacol. 2016;194:131-6. doi: 10.1016/j.jep.2016.09.005
26. Bradley PP, Priebat DA, Christensen RD, et al. Measurement of cutaneous inflammation: estimation of neutrophil content with an enzyme marker. J Invest Dermatol. 1982;78:206-9. doi: 10.1111/1523-1747.ep12506462
27. Bailey PJ. Sponge implants as models. Methods Enzymol. 1988;162:327-34. doi: 10.1016/0076-6879(88)62087-8
28. Cassini-Vieira P, Moreira C, da Silva M, et al. Estimation of wound tissue neutrophil and macrophage accumulation by measuring myeloperoxidase (MPO) and N-Acetyl-□-D-glucosaminidase (NAG) Activities. BIO-PROTOCOL. 2015;5(22):1-7. doi: 10.21769/BioProtoc.1662
29. Artem Ataide J, Caramori Cefali L, Machado Croisfelt F, et al. Natural actives for wound healing: A review. Phytother Res. 2018;32:1664-74. doi: 10.1002/ptr.6102
30. Ribeiro VP, Arruda C, Abd El-Salam M, et al. Brazilian medicinal plants with corroborated anti-inflammatory activities: a review. Pharm Biol. 2018;56:253-68. doi: 10.1080/13880209.2018.1454480
31. De Albuquerque UP, Muniz de Medeiros P, de Almeida ALS, et al. Medicinal plants of the caatinga (semi-arid) vegetation of NE Brazil: a quantitative approach. J Ethnopharmacol. 2007;114:325-54. doi: 10.1016/j.jep.2007.08.017
32. Pastore S, Potapovich A, Kostyuk V, et al. Plant polyphenols effectively protect HaCaT cells from ultraviolet C-triggered necrosis and suppress inflammatory chemokine expression. Ann N Y Acad Sci. 2009;1171:305-13. doi: 10.1111/j.1749-6632.2009.04684.x
33. Kumar D, Ladaniya MS, Gurjar M, et al. Quantification of flavonoids, phenols and antioxidant potential from dropped *Citrus reticulata* blanco fruits influenced by drying techniques. Molecules. 2021;26:4159. doi: 10.3390/molecules26144159

34. dos Santos JS, Monte-Alto-Costa A. Caffeic acid phenethyl ester improves burn healing in rats through anti-inflammatory and antioxidant effects. J Burn Care Res. 2013;34:682-8. doi: 10.1097/BCR.0b013e3182839b1c
35. Song HS, Park TW, Sohn UD, et al. The effect of caffeic acid on wound healing in skin-incised mice. Korean J Physiol Pharmacol. 2008;12:343-7. doi: 10.4196/kjpp.2008.12.6.343
36. Serarslan G, Altuğ E, Kontas T, et al. Caffeic acid phenethyl ester accelerates cutaneous wound healing in a rat model and decreases oxidative stress. Clin Exp Dermatol. 2007;32:709-15. doi: 10.1111/j.1365-2230.2007.02470.x
37. Sami DG, Heiba HH, Abdellatif A. Wound healing models: A systematic review of animal and non-animal models. Wound Medicine. 2019;24:8-17. doi: 10.1016/j.wndm.2018.12.001
38. Thakur R, Jain N, Pathak R, et al. Practices in wound healing studies of plants. Evid Based Complement Alternat Med. 2011;2011:438056. doi: 10.1155/2011/438056
39. Gutiérrez-Grijalva EP, Antunes-Ricardo M, Acosta-Estrada BA, et al. Cellular antioxidant activity and in vitro inhibition of α-glucosidase, α-amylase and pancreatic lipase of oregano polyphenols under simulated gastrointestinal digestion. Food Res Int. 2019;116:676-86. doi: 10.1016/j.foodres.2018.08.096
40. Phillipson M, Kubes P. The healing power of neutrophils. Trends Immunol. 2019;40:635-47. doi: 10.1016/j.it.2019.05.001
41. Goren I, Allmann N, Yogev N, et al. A transgenic mouse model of inducible macrophage depletion: effects of diphtheria toxin-driven lysozyme M-specific cell lineage ablation on wound inflammatory, angiogenic, and contractive processes. Am J Pathol. 2009;175:132-47. doi: 10.2353/ajpath.2009.081002.
42. Mirza R, DiPietro LA, Koh TJ. Selective and specific macrophage ablation is detrimental to wound healing in mice. Am J Pathol. 2009;175:2454-62. doi: 10.2353/ajpath.2009.090248
43. Krzyszczyk P, Schloss R, Palmer A, et al. The role of macrophages in acute and chronic wound healing and interventions to promote pro-wound healing phenotypes. Front Physiol. 2018;9:419. doi: 10.3389/fphys.2018.00419
44. De Moura FBR, Ferreira BA, Deconte SR, et al. Wound healing activity of the hydroethanolic extract of the leaves of *Maytenus ilicifolia* Mart. Ex Reis. J Tradit Complement Med. 2021;11:446-56. doi: 10.1016/j.jtcme.2021.03.003
45. Nosenko MA, Ambaryan SG, Drutskaya MS. Proinflammatory cytokines and skin wound healing in mice. Mol Biol (Mosk). 2019;53:741-54. doi: 10.1134/S0026898419050136
46. Huang S-M, Wu C-S, Chiu M-H, et al. High glucose environment induces M1 macrophage polarization that impairs keratinocyte migration via TNF-α: An important mechanism to delay the diabetic wound healing. J Dermatol Sci. 2019;96:159-67. doi: 10.1016/j.jdermsci.2019.11.004
47. Liechty KW, Kim HB, Adzick NS, et al. Fetal wound repair results in scar formation in interleukin-10-deficient mice in a syngeneic murine model of scarless fetal wound repair. J Pediatr Surg. 2000;35:866-72. doi: 10.1053/jpsu.2000.6868
48. Peranteau WH, Zhang L, Muvarak N, et al. IL-10 overexpression decreases inflammatory mediators and promotes regenerative healing in an adult model of scar formation. J Invest Dermatol. 2008;128:1852-60. doi: 10.1038/sj.jid.5701232
49. Balaji S, Wang X, King A, et al. Interleukin-10-mediated regenerative postnatal tissue repair is dependent on regulation of hyaluronan metabolism via fibroblast-specific STAT3 signaling. FASEB J. 2017;31:868-81. doi: 10.1096/fj.201600856R